A Design Exploration of Natural Laminar Flow Applications for the SUSAN Electrofan Concept

Michelle N. Lynde[1], Richard L. Campbell[2], and Brett R. Hiller[3]
NASA Langley Research Center, Hampton, Virginia, 23681

A trade study supported by the NASA Convergent Aeronautics Solutions (CAS) Project is presently underway to explore the desirability, feasibility, and viability of a new vehicle concept. The vehicle under development is the SUbsonic Single Aft eNgine (SUSAN) Electrofan configuration, which is a subsonic regional jet with the transformative concept of combining wing-mounted distributed electrified aircraft propulsion with a single engine design. The multidisciplinary team is investigating several potential technologies that would help the SUSAN Electrofan configuration achieve its performance goals, one of which is the application of Natural Laminar Flow (NLF) to the main wing. The present computational study utilizes the Crossflow Attenuated Natural Laminar Flow (CATNLF) design method to reshape the wing airfoils to obtain significant extents of NLF at the cruise condition. Fully-turbulent and laminar designs were performed to quantify the aerodynamic performance potential of NLF on the SUSAN Electrofan configuration. The laminar design supported laminar flow on 53% of the area of the wing upper surface, resulting in a 19 count (8.8%) drag reduction for the wing-fuselage configuration. The near-cruise off-design characteristics are also studied and illustrate that the robust laminar design sustains an NLF performance benefit through perturbations in Mach and angle of attack. A discussion is also included on multidisciplinary implications of utilizing NLF for the configuration, including design, manufacturing, and operational considerations required to support NLF on the main wing, as well as the interaction between the potential wing-mounted boundary layer ingestion technology that is also being explored for the SUSAN Electrofan configuration.

Nomenclature

Acronyms

BLI	=	Boundary Layer Ingestion
BLSTA3D	=	Boundary Layer code for Stability Analysis 3D, boundary layer profile solver
CAS	=	Convergent Aeronautics Solutions
CATNLF	=	Crossflow Attenuated Natural Laminar Flow
CDISC	=	Constrained Direct Iterative Surface Curvature, design module
CF	=	Crossflow
CFD	=	Computational Fluid Dynamics
CRM	=	Common Research Model
CRM-NLF	=	Common Research Model with Natural Laminar Flow
DEP	=	Distributed Electric Propulsion
LA	=	Laminar Analysis
LASTRAC	=	Langley Stability and Transition Analysis Code, transition prediction software
LST	=	Linear Stability Theory
MAC	=	Mean Aerodynamic Chord
NASA	=	National Aeronautics and Space Administration
NF	=	N-Factor
NLF	=	Natural Laminar Flow
SA	=	Spalart-Allmaras

[1] Research Aerospace Engineer, NASA Langley Research Center, Configuration Aerodynamics Branch, AIAA Member.
[2] Senior Research Engineer, NASA Langley Research Center, Configuration Aerodynamics Branch, AIAA Associate Fellow.
[3] Research Aerospace Engineer, NASA Langley Research Center, Configuration Aerodynamics Branch, AIAA Member.

SUSAN = SUbsonic Single Aft eNgine
TetrUSS = Tetrahedral Unstructured Software System, flow solver package
TA = Turbulent Analysis
TS = Tollmien-Schlichting
USM3D = Unstructured Mesh 3D, Navier-Stokes flow solver

Symbols
α = Angle of attack, degrees
c = Chord length, feet
c_f = Sectional skin friction coefficient
c_l = Sectional lift coefficient
c_m = Sectional pitching moment coefficient
C_L = Total vehicle lift coefficient
C_D = Total vehicle drag coefficient
C_m = Total vehicle pitching moment coefficient
C_P = Pressure coefficient
D = Drag, lb_f
L = Lift, lb_f
M = Mach number
Re_θ = Reynolds number based on attachment line boundary layer momentum thickness
Re_c = Reynolds number based on local chord length
Re_{MAC} = Reynolds number based on mean aerodynamic chord
$(r/c)_{LE}$ = Leading-edge radius nondimensionalized by local chord
x/c = x-location nondimensionalized by local chord
$(x/c)_t$ = x-location of transition nondimensionalized by local chord
η = Semispan location nondimensionalized by semispan length
Λ_{LE} = Leading-edge sweep, degrees

I. Introduction

AIRCRAFT designers are continually pursuing technology that enables significant performance improvements and emissions reductions. The SUbsonic Single Aft eNgine (SUSAN) Electrofan project aims to develop a configuration that incorporates novel propulsion technology to meet these ambitious emissions goals. The SUSAN Electrofan aircraft, shown in Figure 1, is a subsonic regional jet with the transformative concept of combining wing-mounted distributed electrified aircraft propulsion with a single engine design. The trade study, currently being conducted by a multidisciplinary team of NASA engineers as part of the NASA Convergent Aeronautics Solutions (CAS) project, focuses on reducing fuel usage, emissions, and cost, while utilizing existing airport infrastructure and being flight certifiable. Figure 2 highlights several key features of the vehicle presently being studied by the team. The airframe is a classical tube and wing with T-tail architecture sized for 180 passengers. There are two wing technologies under consideration, including Natural Laminar Flow (NLF) and wing-mounted Boundary Layer Ingestion (BLI) distributed electric propulsion (DEP). The present layout has 8 DEP systems per wing for a total of 16 electric engines providing a substantial portion of the vehicle total thrust. The single engine mounted on the fuselage centerline near the tail will also utilize BLI. This turbofan will provide a portion of the required vehicle thrust as well as shaft power for the main generators. Three thermal management loops at different temperatures are used to manage the engine, electrical system, and batteries. Additional details on the SUSAN Electrofan configuration and the associated trade study are reported in the companion paper titled "Subsonic Single Aft Engine (SUSAN) Transport Aircraft Concept and Trade Space Exploration" by R. Jansen et al. [1].

Figure 1. Conceptual design of the SUSAN Electrofan configuration.

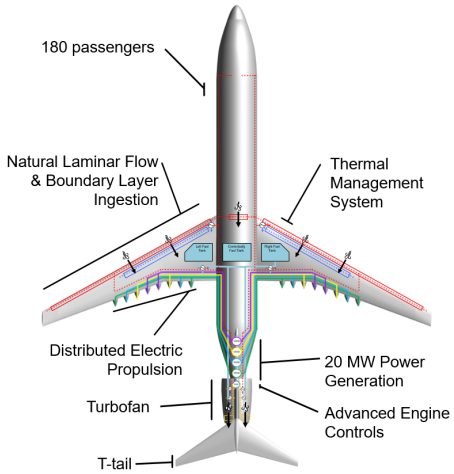

Figure 2. Key features of the SUSAN Electrofan configuration.

In addition to incorporating hybrid-electric propulsion technology, the SUSAN Electrofan project is investigating additional methods to improve the vehicle performance. One such technology is the application of NLF through aerodynamic design. Laminar flow provides a performance improvement through the reduction of skin friction and profile drag. Laminar flow on the main wing upper surface offers the largest potential for drag reduction due to the higher skin friction levels in that region. However, the main wings of transport vehicles have historically been a challenge to obtain laminar flow because of the presence of crossflow instabilities that are amplified with higher wing sweep and higher Reynolds numbers. The present SUSAN Electrofan computational study investigates NLF benefits on the main wing by utilizing the NASA design method, referred to as Crossflow Attenuated Natural Laminar Flow (CATNLF). The CATNLF design method reshapes the wing airfoils to obtain pressure distributions known to reduce crossflow growth at the leading edge [2-3]. The CATNLF method has been utilized in several computational studies, and was experimentally investigated in a wind tunnel test to validate the computational results [4-6]. One of the notable advantages of using the CATNLF method to investigate the NLF potential during this trade study is that the method relies simply on airfoil shaping to obtain laminar flow extents, instead of historic methods, such as sweep reduction or a suction system. The airfoil shaping is a localized change that has minimal impact to other technology studies occurring simultaneously for the SUSAN Electrofan project. The CATNLF method does not require complex systems that add weight or storage challenges, or change the cruise speed of the configuration that can impact the mission profile.

This paper documents the performance impact of including NLF on the main wing of the SUSAN Electrofan configuration. The study includes two redesigned wings, one turbulent design to serve as a comparable baseline, and one laminar design using the CATNLF method. High-fidelity Computational Fluid Dynamics (CFD) analyses are utilized to quantify any aerodynamic performance differences between the designed configurations. A discussion is also included on the potential impact an NLF wing would have on other technologies considered in this multidisciplinary trade study or aircraft requirements.

II. Design and Analysis Approach

The exploratory study of applying NLF to the SUSAN Electrofan configuration utilizes a suite of computational tools, including a flow solver, design code, and transition prediction software. The workflow of the computational tools is illustrated in Figure 3. The flow solver used in this work is NASA's USM3D, a Reynolds-averaged Navier-Stokes solver [7]. This flow solver uses unstructured multielement grids, and the solutions for this work were obtained using the standard Spalart-Allmaras (SA) turbulence model with negative provisions. The grids used for this study were all tetrahedral for compatibility with the design module. The forced-laminarization feature was also used to suppress turbulence production in the regions predicted to support laminar flow on the laminar design configuration. The flow solver was coupled with the design code, Constrained Direct Iterative Surface Curvature (CDISC) [8]. CDISC is a knowledge-based design tool that alters the shape of an aerodynamic surface to produce analysis pressures that closely match a target pressure distribution. This tool has been widely used for the aerodynamic design of configurations for computational studies, wind tunnel models, and flight test efforts over the past several decades. Recently, CDISC was the design tool that has enabled the development of the CATNLF design method. The CATNLF method, which is being applied in this study to the SUSAN Electrofan configuration, requires the use of transition prediction software. The

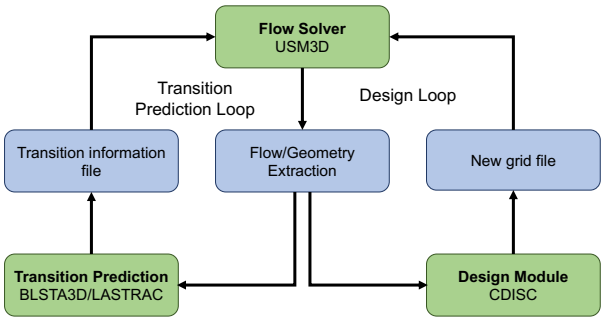

Figure 3. Flow chart of the CDISC design and analysis process.

BLSTA3D boundary layer profile solver estimates the velocity and temperature profiles from the flow solver pressure distributions [9]. These boundary layer profiles are then passed to the stability analysis code, LASTRAC, which calculates the growth of both Tollmien-Schlichting (TS) and crossflow (CF) modal instabilities [10]. For this work, the stability analysis calculations are based on the Linear Stability Theory (LST) e^N method with compressibility effects included and no curvature effects. The TS and CF growths are used to provide a predicted extent of laminar flow based on a user-prescribed critical N-factor. The critical N-factor for this work is chosen to be 10 to represent a flight environment.

The CATNLF method was developed to provide significant extents of laminar flow on the wings of typical transports that have previously been limited by crossflow transition due to the high sweep and high Reynolds numbers of those components. The method was developed in computational studies on both transonic and supersonic transports prior to being used to design the Common Research Model with Natural Laminar Flow (CRM-NLF) that was experimentally investigated in the National Transonic Facility in 2018 [4-6]. The method relies on pressure gradients to control the growth of both CF and TS instabilities. Figure 4 shows a sample CATNLF pressure distribution for a transonic wing compared to a typical turbulent pressure distribution with notable differences identified with red arrows. The rapid acceleration seen at the leading edge of the laminar pressure distribution is the primary mechanism for controlling CF growth. Due to the sweep and Reynolds numbers of typical transport wings, CF is still expected to grow at the leading edge, but the rapid acceleration reduces the amount of growth such that the associated CF N-factors remain subcritical. Aft of the leading edge, a notable difference can be observed in the C_P gradients of the turbulent and laminar pressure distributions. CATNLF utilizes a mild favorable pressure gradient to control the TS growth, while a turbulent design has a mild adverse gradient to reduce shock strength. The primary objective of this region for a laminar design is to gradually grow the TS from the leading edge to the desired transition location, typically just ahead of the shock. Due to the favorable pressure gradient required to control TS growth, the shock strength of CATNLF airfoils are often greater than that of comparable turbulent airfoils. However, the drag benefits associated with laminar flow typically outweigh the wave-drag penalty from the increased shock strength. This paper focuses on comparing laminar and turbulent wing designs to quantify the approximate performance differences between the two designs for the SUSAN Electrofan configuration to determine the potential performance impact if the configuration included NLF wings.

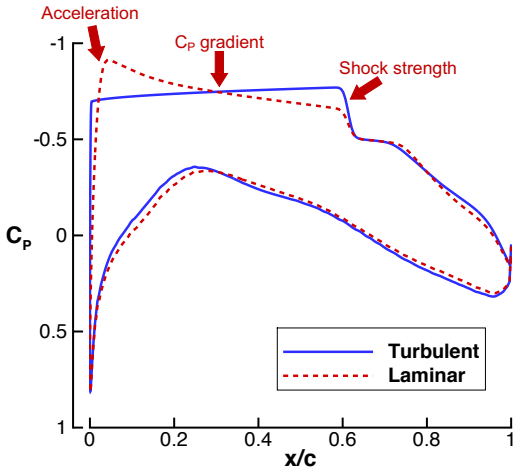

Figure 4. Example transonic transport pressure distribution for both turbulent and laminar wings. Notable differences of the pressure distributions are identified.

III. Design Results

The two aerodynamic wing designs presented in this paper are based on the most recent SUSAN Electrofan sizing and flight conditions with the knowledge that the team is concurrently performing technology trade studies that may alter the reference design conditions and configuration details as the design matures. The intent of the designs in this paper is to quantify the potential increment in performance due to NLF technology. As such, design decisions were made for this work that supported this objective while keeping the design as simple as possible to reduce complexity and computational cost. This section presents the design strategy, cruise point design results for both the turbulent and laminar wing designs, and discuss differences between the two designs at cruise point and off-design conditions.

A. Design Setup

The current design condition for the configuration is Mach 0.785, at an altitude of 37,000 ft, and a lift coefficient (C_L) of 0.5. The configuration has a mean aerodynamic chord (MAC) of 13.37 ft, which produces a Reynolds number based on the MAC (Re_{MAC}) of 23.1 million at the design point. For this study, a simplified wing-body geometry was used to reduce the required computational resources enabled by a smaller grid. All propulsion, including the planned distributed electric propulsion on the wing and the tail cone thruster on the fuselage, were removed from this geometry for simplification. While the planned distributed electric propulsion on the wing is expected to significantly impact the wing aerodynamics, the propulsion design had not yet been finalized to be included in this work. Additionally, keeping a clean wing for this study offers the opportunity to directly study the impact of NLF without the added complexity of propulsion airframe integration effects. Discussions on the trades required to achieve NLF, as well as the potential impact of distributed electric propulsion to the NLF potential, are presented in the following section, "Multidisciplinary Considerations for Implementing NLF".

The all-tetrahedral grid used for this work was 44.4 million cells with an average y+ value of 0.5 and had increased refinement in the wing leading-edge region. For the CDISC design, 11 chordwise design stations were created along the wing semispan, as shown in Figure 5. The four stations highlighted in red will be used as examples for this paper. General parameters for the four example stations are shown in Table 1.

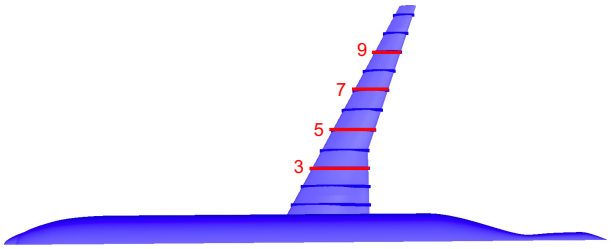

Figure 5. Planform view of the SUSAN Electrofan wing-body configuration with 11 CDISC design stations.

Table 1. General parameters for the four example stations.

Station	η	Chord (ft)	Re_c (million)
3	0.29	13.68	23.6
5	0.45	10.35	17.9
7	0.62	8.47	14.6
9	0.79	6.60	11.4

The baseline wing for the SUSAN Electrofan configuration is a previously optimized wing from a similarly sized NASA transport concept. Several constraints were implemented for both the turbulent and laminar CDISC designs. The spanwise lift distribution was maintained as closely as possible and the maximum thickness was held constant. Curvature constraints were included to help maintain reasonable off-design performance and to avoid transition due to Görtler vortices on the laminar design. For both designs, the flow constraints used to define the target pressure distribution relied on the default best-practice values within the CDISC design tool. The turbulent design has target pressure distributions that aimed to reduce wave drag, primarily by introducing an adverse pressure gradient and aft loading to reduce the shock strength. The laminar design target pressure distributions followed the CATNLF design methodology as discussed previously. Both the turbulent and laminar designs were started from the same baseline geometry and showed reasonable agreement to the target pressures across the span of the wing after 60 design cycles.

The CDISC design process provides a single-point design such that the target pressures and airfoil shaping correspond to one specific flow condition. As mentioned, the primary cruise condition is used for the design point for the SUSAN Electrofan wing designs. One inherent risk of utilizing a single-point design tool is the chance of significant performance degradation at off-design conditions because the design process does not include analysis at off-design conditions. To protect against significant off-design performance loss, design constraints are implemented in CDISC to avoid specific geometry or flow features that are known to lead to adverse performance off-design. Examples of some multipoint design constraints implemented in CDISC include a maximum curvature limit to avoid undesirable shock characteristics at off-design conditions and a maximum adverse pressure gradient limit to avoid flow separation at off-design conditions. The subsequent subsection will present the design results from the cruise point condition, followed by an assessment of the off-design characteristics of the designs.

B. Cruise Point Design Results

The first step toward quantifying the NLF potential on the SUSAN Electrofan configuration is designing the baseline wing geometry to be a well-performing turbulent wing for the transonic cruise point. This turbulent wing will

provide a new turbulent baseline for comparisons with the laminar design, which is necessary to eliminate any potential differences in performance due to design strategy.

Figure 6 shows the pressure distributions and airfoil shapes relevant to the turbulent design for the four example stations. The pressure plots compare the baseline configuration, the turbulent target pressures generated by CDISC, and the final turbulent design. The good agreement between the final design pressures and the CDISC target pressure distributions suggests the design process was successful in producing a geometry that provides the desired flow features. The design was successful in eliminating the multiple shocks seen in the baseline pressures and introducing an adverse pressure gradient that allows for a single shock of reduced strength. The resulting airfoils display many characteristics of a standard supercritical airfoil while maintaining important baseline parameters like maximum thickness.

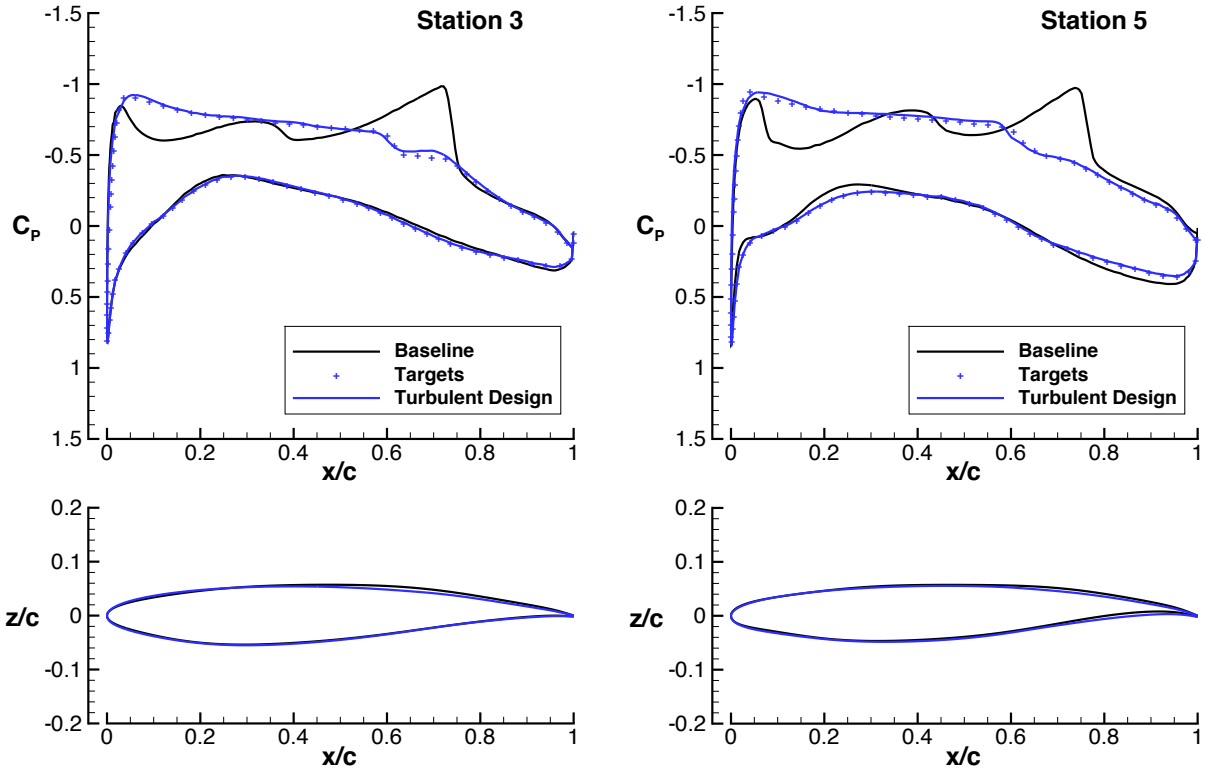

a. Station 3 pressures (top) and airfoil (bottom). **b. Station 5 pressures (top) and airfoil (bottom).**

Figure 6. Pressures and airfoils from the baseline, CDISC targets, and turbulent design.

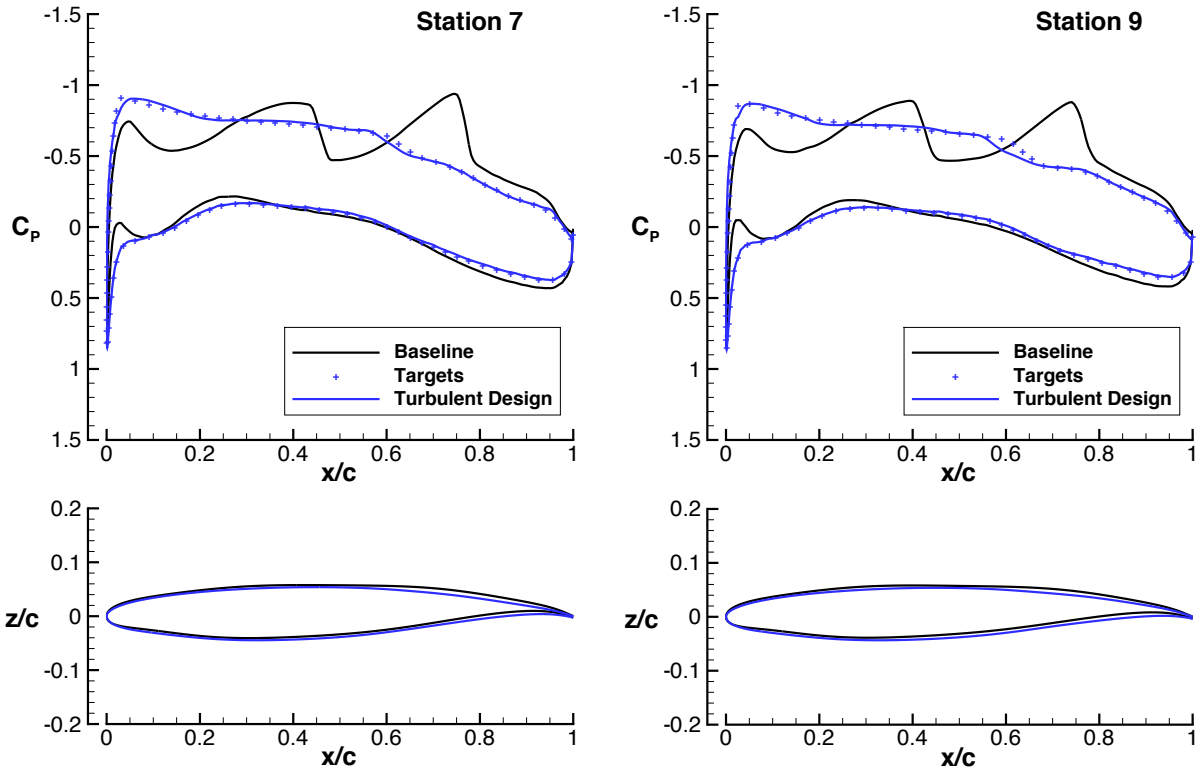

c. Station 7 pressures (top) and airfoil (bottom). **d. Station 9 pressures (top) and airfoil (bottom).**

Figure 6 (cont.). Pressures and airfoils from the baseline, CDISC targets, and turbulent design.

The completed turbulent wing design serves as the new comparison vehicle used to quantify the NLF performance increment available to the SUSAN Electrofan configuration. The laminar design was conducted for identical cruise point conditions, run for the same number of design cycles, and analyzed to similar CFD convergence levels on the same baseline CFD grid as the turbulent design. The CFD during the laminar design process was kept fully turbulent (i.e., no laminar flow extents were included in the flow analysis) to improve the off-design characteristics. Results from previous studies have suggested that keeping the flow analysis fully turbulent during the design process reduces the wave-drag penalty if laminar flow is lost on a CATNLF design. Once the design is complete, stability analysis results are acquired to predict the extent of laminar flow on the design, and then the configuration is reanalyzed in CFD with the appropriate extents of laminar flow in the solver. For this paper, the laminar wing with a Turbulent Analysis (TA) will be labeled as "Laminar Design (TA)", and the laminar wing with a Laminar Analysis (LA) will be labeled as "Laminar Design (LA)".

The pressure distributions and airfoils from the Turbulent Design and Laminar Design (TA) are shown in Figure 7 and illustrate the required differences needed to obtain significant extents of NLF. A rapid acceleration at the leading edge was introduced in the laminar design to control CF instabilities on the wing. Additionally, the upper surface pressure gradient was altered from the turbulent adverse gradient used to reduce shock strength to a slightly favorable gradient in the laminar design to control TS instabilities. Several features were kept constant to try to isolate the impact of NLF, such as shock location and aft loading. The laminar design airfoil shapes maintained the characteristics of a supercritical airfoil. Minimal shape changes were required to obtain the CATNLF pressures, but the laminar design does show slightly reduced leading-edge radius on the inboard stations. This reduction in leading-edge radius helps accelerate the flow quickly to control CF growth.

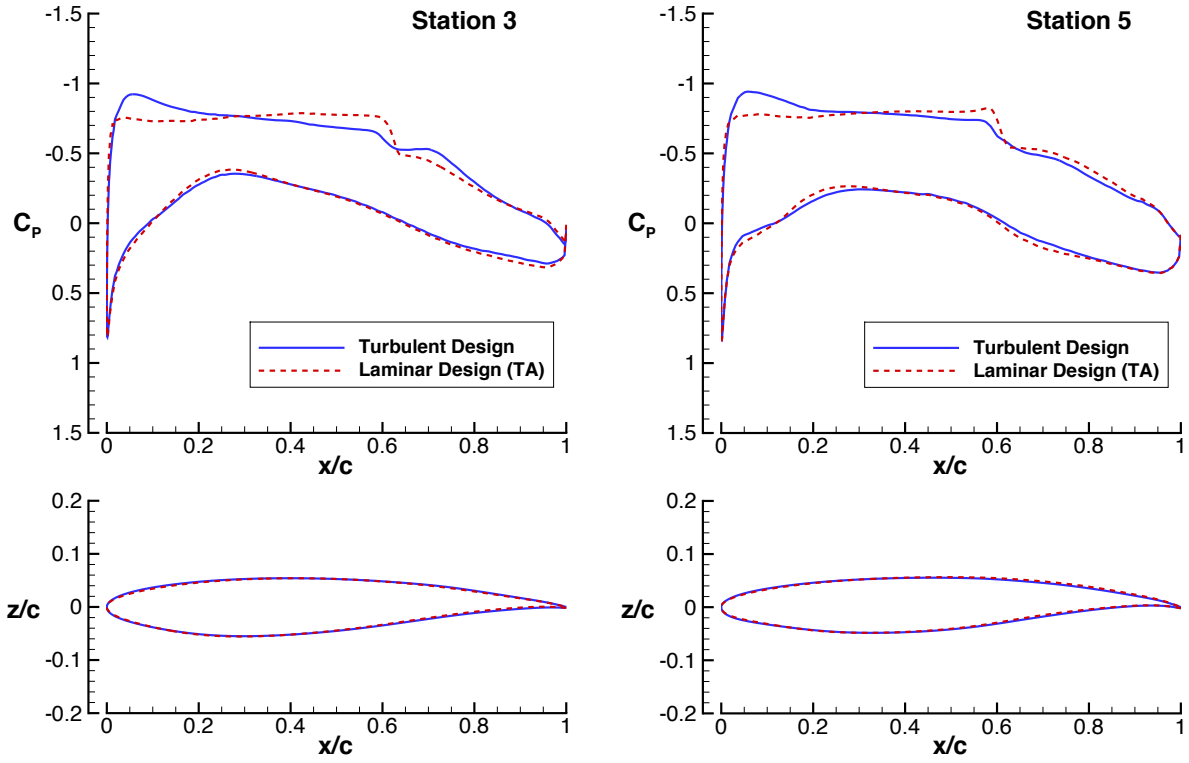

a. Station 3 pressures (top) and airfoil (bottom).

b. Station 5 pressures (top) and airfoil (bottom).

c. Station 7 pressures (top) and airfoil (bottom).

d. Station 9 pressures (top) and airfoil (bottom).

Figure 7. Pressures and airfoils from the laminar and turbulent design.

Once the Laminar Design (TA) was completed, the wing was analyzed using stability analysis to predict the transition locations on the configuration. The CF and TS N-factor (NF) growth from the 4 example stations are shown in Figure 8. Across the span, the CF has been successfully suppressed due to the rapid acceleration introduced in the CATNLF pressures. The CF still grows at the leading edge, but remains subcritical such that no transition is expected due to CF. Inboard, where the Reynolds number is higher, the maximum CF value at the leading edge is significantly higher. The TS gradually grows from the leading edge to the desired transition location just forward of the shock. This gradual growth enables smaller changes in laminar flow extent if the freestream turbulence levels produce a lower critical N-factor. The Reynolds number based on attachment-line momentum thickness (Re_θ) stayed below 235 across the span of the wing, indicating the wing should avoid any attachment line transition according to Poll's criteria [11]. At the inboard stations, the Re_θ reached 100, which is expected to relaminarize the attachment line boundary layer to protect from contamination from the turbulent fuselage. This strategy of attachment line relaminarization with low Re_θ values was successful in the recent CRM-NLF wind tunnel experiment [4-5]. However, additional protection against attachment-line contamination may be desired in the form of a device that diverts the fuselage boundary layer away from the leading edge of the wing, such as a Gaster bump or slot [12]. The Laminar Design is predicted to support NLF on 53% of the surface area of the wing upper surface, as shown in the planform view of the transition front in Figure 9.

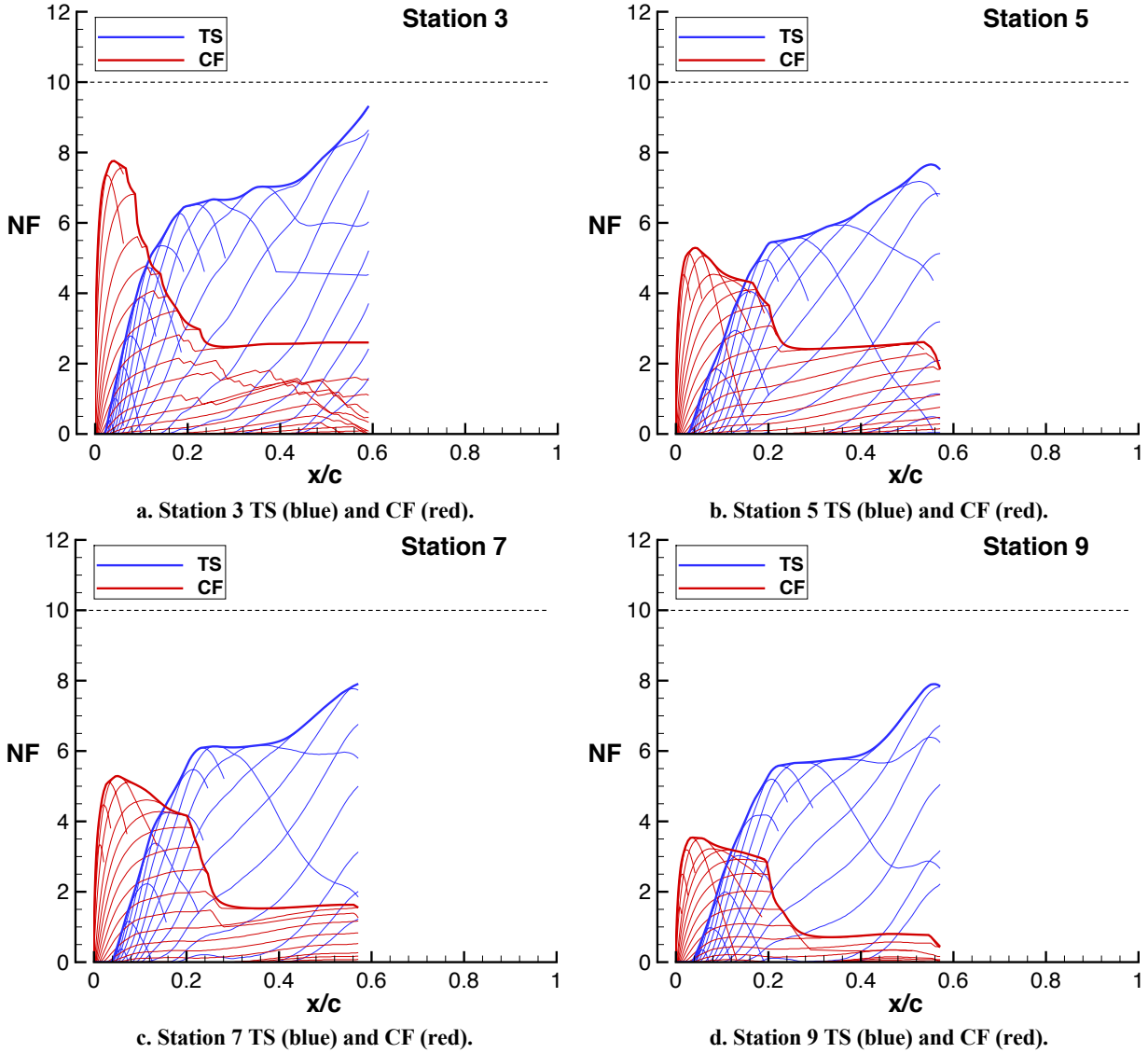

a. Station 3 TS (blue) and CF (red).

b. Station 5 TS (blue) and CF (red).

c. Station 7 TS (blue) and CF (red).

d. Station 9 TS (blue) and CF (red).

Figure 8. TS and CF instability growth for the laminar design configuration.

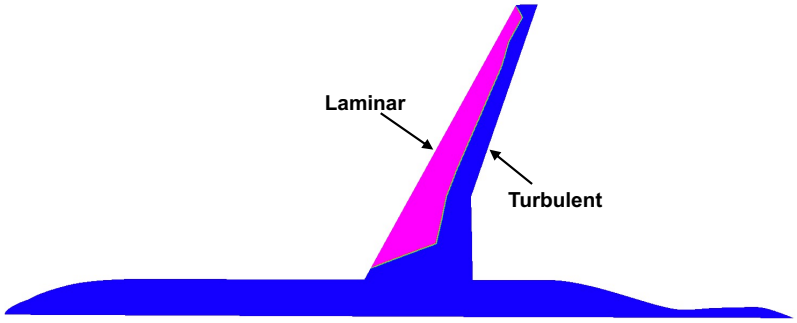

Figure 9. Planform view of the laminar design wing showing the predicted transition front at the design condition.

The predicted extents of laminar flow obtained from the above analysis were used in the CFD to appropriately model NLF on the wing. This solution, labeled "Laminar Design (LA)", is considered the final laminar design. The Laminar Design (TA) solution obtained during the design process represents the vehicle aerodynamics if all laminar flow was lost. This total loss of laminar flow would be a result of extreme changes in either surface finish or freestream turbulence conditions. This Laminar Design (TA) represents the worst-case scenario for NLF, however, it is more likely that laminar flow would be lost gradually, resulting in performance somewhere between the Laminar Design (LA) and Laminar Design (TA) solutions. Figure 10 compares the pressure and skin-friction distributions from a C_L-matched solution of both the turbulent analysis and laminar analysis of the Laminar Design wing. The Laminar Design (LA) shows further aft shocks and several stations show a small region of acceleration ahead of the shock, which increases shock strength. The aft loading is slightly increased in the LA solution due to the thinner boundary layer, which increases the effective camber of the airfoil. The skin-friction distributions show the reduced skin-friction characteristic of laminar flow on the LA solution upper surface. A rapid increase in skin friction is seen aft of the transition location. The lower surface skin friction remains constant between the two solutions because this design did not include lower surface laminar flow.

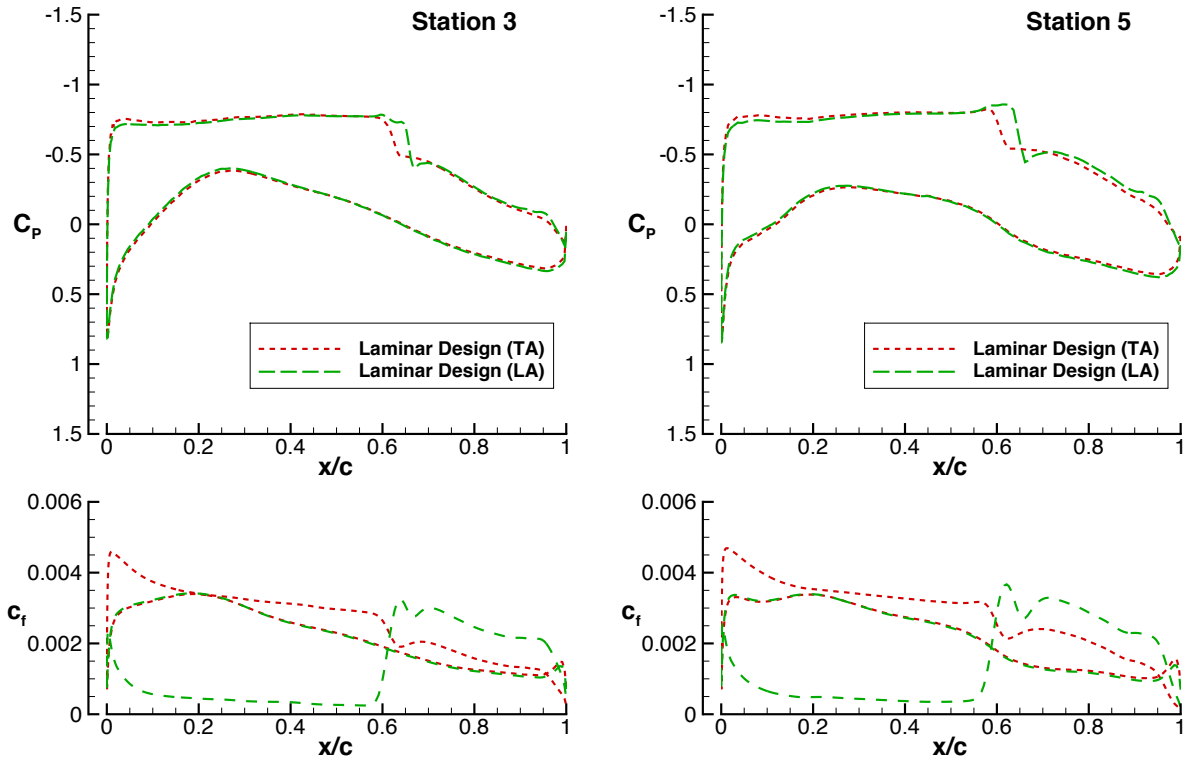

a. Station 3 pressures (top) and skin friction (bottom).

b. Station 5 pressures (top) and skin friction (bottom).

Figure 10. Pressure and skin-friction distributions for the laminar design comparing flow solutions with turbulent analysis (TA) and laminar analysis (LA).

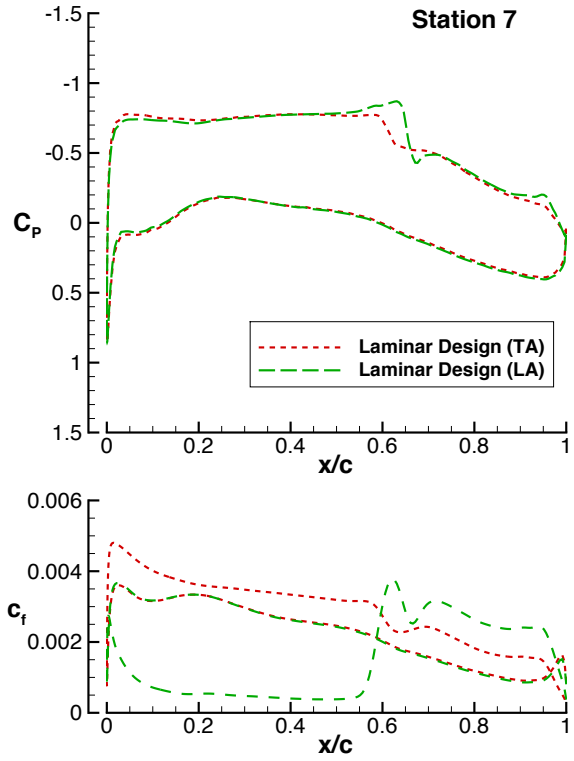

c. Station 7 pressures (top) and skin friction (bottom).

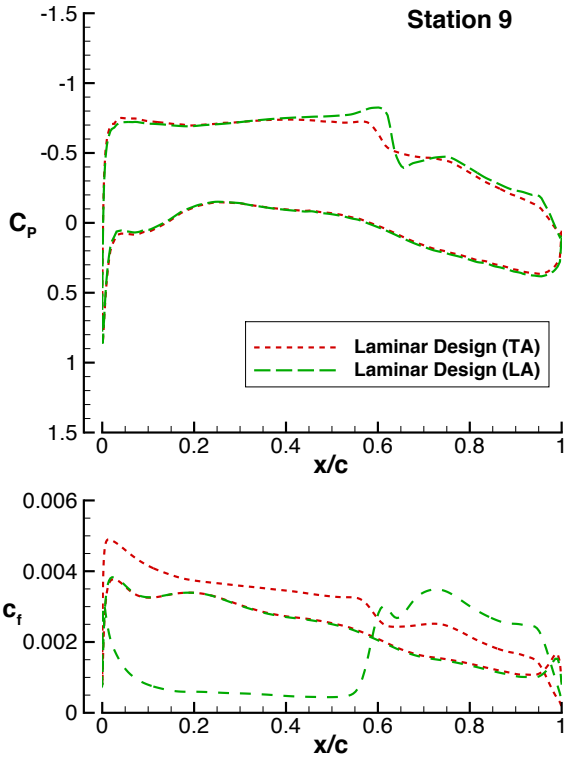

d. Station 9 pressures (top) and skin friction (bottom).

Figure 10 (cont.). Pressure and skin-friction distributions for the laminar design comparing flow solutions with turbulent analysis (TA) and laminar analysis (LA).

Spanwise characteristics of the Turbulent Design and Laminar Design (LA) are shown in Figure 11. The sectional lift distribution was held relatively constant throughout the design process to maintain wing loading character, such as induced drag or root bending moment. The increased pitching moment for the Laminar Design was enabled by the thinner boundary layer from laminar flow, which makes a more rapid pressure recovery at the trailing edge possible while avoiding separation. The further aft shock on the Laminar Design also contributed to the increased pitching moment. A trim drag analysis would be required to evaluate the performance impact of the altered pitching moment. The leading-edge radius was free to change during the Laminar Design to help obtain the desired CATNLF pressure distributions. The Laminar Design required smaller radii inboard on the wing, where CF grows more rapidly due to the high Reynolds numbers, in order to accelerate the flow more rapidly. That reduced leading-edge radius was no longer required outboard where CF is less of a challenge, so the design produced larger radii outboard. For the Turbulent Design, the leading-edge radius was set as a function of the maximum thickness according to the CDISC best practices established from other design work. The twist for both configurations shows similar behavior and were both smoothed to provide more gradual changes in wing geometry across the span.

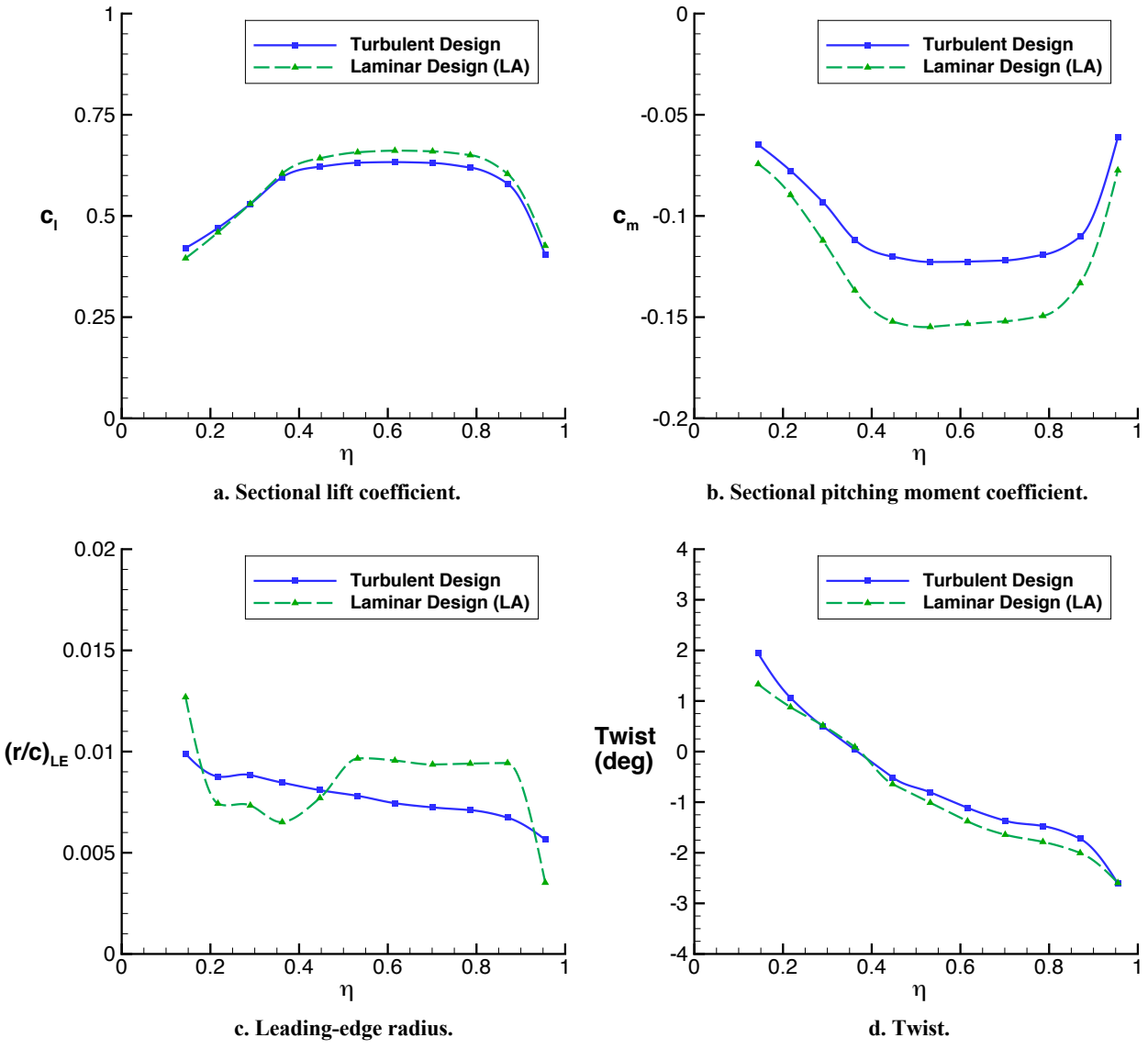

a. Sectional lift coefficient.

b. Sectional pitching moment coefficient.

c. Leading-edge radius.

d. Twist.

Figure 11. Spanwise distributions of sectional lift, sectional pitching moment, leading-edge radius, and twist for the Turbulent Design and Laminar Design (LA).

The goal of the study was to identify the potential performance benefit of NLF when applied to the main wing on the SUSAN Electrofan configuration. The force and moment data from the flow solver are utilized to quantify any performance differences between the different wing-body designs. Table 2 compares the baseline geometry, turbulent design, and laminar design. The laminar design was also analyzed with no laminar flow modeled in the flow solver, labeled "Laminar Design (TA)", in order to identify the performance changes that could be encountered if somehow all laminar flow is lost. This analysis is representative of a worst-case scenario for the design. A partial loss in laminar flow is more likely due to nonideal conditions, such as surface imperfections creating turbulent wedges or a change in environmental turbulent flow conditions causing a forward shift in transition front. A partial loss in laminar flow would perform somewhere between the Laminar Design (LA) and the Laminar Design (TA) results.

Table 2. Force and moment data for the wing-body designs at the design condition of M = 0.785, Alt. = 37,000 ft, Re_{MAC} = 23.1 million, and C_L = 0.5.

Configuration	α (deg)	C_L	C_D	C_m	ML/D
Baseline	2.51	0.500	0.0229	-0.290	17.14
Turbulent Design	2.10	0.500	0.0216	-0.281	18.17
Laminar Design (LA)	1.79	0.500	0.0197	-0.309	19.92
Laminar Design (TA)	2.10	0.500	0.0216	-0.291	18.17

The force and moment data show that the Turbulent Design acquired using CDISC would provide a 13-count (5.7%) drag reduction compared to the previously optimized Baseline wing. This drag reduction highlights the importance of performing a turbulent design first, to eliminate any performance differences originating from design tool or strategy differences. The Laminar Design (LA) further reduced the drag by 19-counts (8.8%) compared to the Turbulent Design. This represents the performance potential at the cruise condition design point for a laminar design compared to a turbulent design performed with a similar tool. The Laminar Design (TA) data shows that even if all laminar flow was lost on the wing, there would be no performance penalty compared to the Turbulent Design. Previous studies using the CATNLF design method showed a larger performance penalty between a turbulent design and a laminar design analyzed with no laminar flow than seen in this SUSAN Electrofan configuration study. This penalty often originates from the stronger shocks on laminar designs that come from the favorable pressure gradient required for NLF. The increased wave drag from these stronger shocks is typically outweighed by the reduced skin-friction drag from NLF (as seen in the 19-count drag reduction when NLF is included). However, in the worst-case scenario when all NLF is lost, the increased wave drag is expected to cause a traditional turbulent design to perform better than a wing designed for laminar flow. The relatively low C_L used in this design study is a possible explanation for why the Laminar Design (TA) did not have as significant of a performance penalty compared to previous CATNLF studies. If the design C_L is increased, the shock strengths would likely increase and cause a larger wave drag difference between the turbulent and laminar designs. It is important to note that the percent differences shown in this work are based on the total drag associated with a wing-fuselage configuration. As additional components are added, the total drag would increase, which would reduce the percent benefit from the NLF wing. In addition, several multidisciplinary factors would need to be taken into account to achieve laminar flow on the main wing. These considerations are discussed in the following section. The aerodynamic force and moment data generated by this study provide a potential performance increment if the wing were designed to support NLF at the cruise condition. These data can be used to help guide the configuration layout decisions and provide a first-look at evaluating if NLF is a worthwhile and compatible technology to include on the SUSAN Electrofan aircraft.

C. Off-Design Results

It is important to consider any impact on aerodynamic behavior of the vehicles at off-design conditions when evaluating the NLF potential. A common concern with NLF designs is that they are more sensitive to off-design conditions because, if small changes in flow conditions resulted in large loss of laminar flow, significant performance penalties would occur. For this study, the off-design assessment was focused on evaluating near-cruise conditions, including small perturbations in C_L and Mach number.

A polar at the cruise Mach number of 0.785 was obtained for the two designed wings. For the Laminar Design, both the Laminar Analysis (LA) and Turbulent Analysis (TA) are considered. An angle-of-attack range from 1.5 to 3.5 degrees was used to adequately cover the near-cruise C_L values, as shown in Figure 12. Across the analyzed range, the Laminar Design (LA) showed performance improvement when compared to both the Laminar Design (TA) and Turbulent Design, indicating there are substantial laminar flow extents at every angle of attack considered that produced reduced drag. The figure labels the values for +/-10% $C_{L,Design}$ to highlight the range of conditions most likely to be experienced during cruise flight. Another relevant off-design condition for consideration is buffet, often

evaluated at 1.3 times $C_{L,Design}$. At this highly loaded condition, the Laminar Design (LA) continues to show extents of laminar flow that produce significant drag reduction, and the solutions showed no signs of early buffet.

In addition to changes with angle of attack, it is desirable for the vehicle to perform well across a wide range of Mach numbers. Figures 13 and 14 show performance characteristics of the configurations at Mach numbers from 0.70 to 0.85. The laminar bucket is clearly distinguishable in the Laminar Design (LA) drag rise curve, with the largest performance benefit near the design Mach number of 0.785. The spread between Laminar Design (LA) and Laminar Design (TA) is due to the performance impact of NLF. The reduction in drag with laminar flow is visibly smaller at the lower Mach numbers compared to the higher Mach numbers. This is primarily due to the loss of laminar flow at the lower Mach numbers. The lower Mach numbers produced rounded leading-edge pressures that did not adequately suppress CF growth, so the majority of the inboard wing at lower Mach numbers transitioned very near the leading edge. Even with the loss of laminar flow at low Mach numbers, the Laminar Design (LA) still reduced drag across the range of Mach numbers analyzed compared to both the Turbulent Design and Laminar Design (TA). The Laminar Design (LA) also demonstrates a higher drag-divergence Mach number compared to the Turbulent Design. As the Mach numbers increases, the Turbulent Design performs notably better than the Laminar Design (TA). This is likely due to the increased shock strengths at these conditions leading to a larger wave drag difference since the Turbulent Design was specifically designed to reduce wave drag and laminar flow often increases wave drag. Figure 14 shows similar performance conclusions for the ML/D curves, with the Laminar Design (LA) providing the highest efficiency, measured as ML/D, across the Mach range.

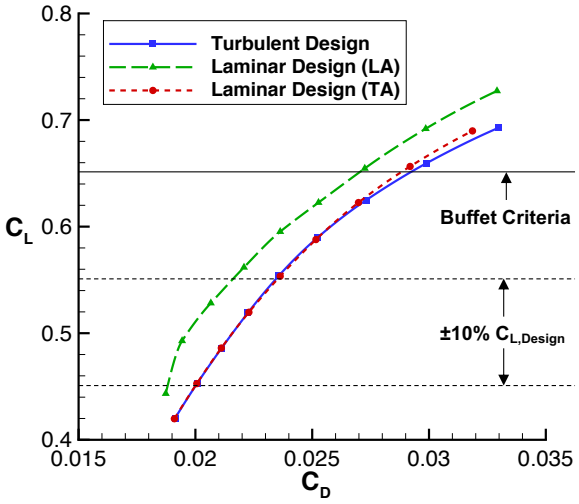

Figure 12. Near-cruise polar comparing the designed configurations.

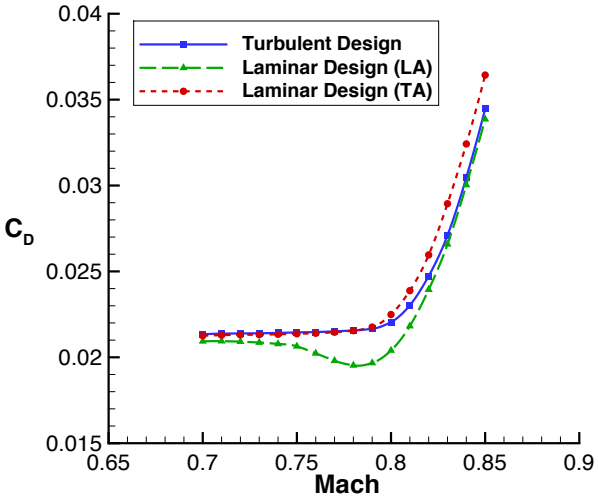

Figure 13. Drag rise curve comparing the designed configuration.

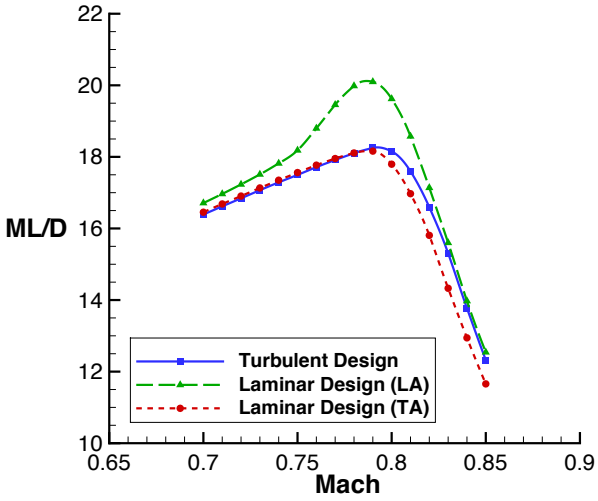

Figure 14. ML/D curve comparing the designed configuration.

The results from the off-design assessment indicate the laminar design has a performance benefit across the near-cruise conditions evaluated. This suggests the design is robust and does not pose significant risk of performance loss at off-design conditions via premature transition. However, if all laminar flow was lost on the laminar design, there is a slight performance penalty expected compared to the turbulent design. In operation, loss of laminar flow is expected to occur in small sections from localized contamination, such as bug strikes or surface imperfections. This more

gradual loss in laminar flow would result in a vehicle that performs somewhere between the Laminar Design (LA) and the Laminar Design (TA) curves.

IV. Multidisciplinary Considerations for Implementing NLF

The aerodynamic results from these designs suggest NLF has significant potential to improve the performance of the SUSAN Electrofan configuration. For the trade study, it is advantageous to understand any potential impact adding NLF may have on the vehicle or other technology being considered. This section will discuss some multidisciplinary considerations or trades that result from implementing NLF on the main wing of the SUSAN Electrofan configuration.

Small surface imperfections can create localized bypass transition by tripping the boundary layer. This necessitates a smoother surface finish for components that support laminar flow compared to a standard turbulent component. This smooth surface requirement can impact several factors over the lifecycle of an aircraft. During the detailed design of the aircraft, this smooth surface requirement would impact the choices for high-lift devices. Traditional leading-edge high-lift devices, such flaps and slats, would cause a step and/or gap on the upper surface of the wing even when stowed during cruise flight. When laminar flow is targeted, the high-lift devices must be designed to avoid any part lines on the wing upper surface, similar to a Kruger flap that is stowed and deployed from the wing lower surface. Additionally, any access panels for maintenance or fueling would be limited to the lower surface. Depending on manufacturing technique, additional attention or time may be required to eliminate part lines and obtain the required surface finish. During operation, the wing upper surface would need to be kept clean, potentially requiring additional servicing to remove any undesired surface imperfections that occur during flight, such as rock or insect strikes. One possible solution under development aims to prevent the accumulation of surface imperfections during flight by adding a protective coating that prevents the adhesion of contaminants [13]. Routine cleaning or the addition of a protective coating may add to the overall manufacturing or operational cost for a vehicle and should be considered when determining the viability of NLF on the wing. Several aircraft are currently flying with NLF on smaller components, such as winglets and nacelles, which suggests the industry has deemed the performance benefit afforded from NLF outweighs these additional considerations for manufacturing and operational changes on the smaller components. The performance benefit is increased with laminar flow on the main wing, but these challenges would likely also increase due to the larger size of the wing compared to the existing NLF examples.

The manufacturing and operational challenges associated with laminar flow wings are similar across most vehicles. An objective of this study was to identify any unique challenges, trades, or configuration impact from implementing NLF technology specifically on the SUSAN Electrofan vehicle. The SUSAN Electrofan team is considering two wing technologies: NLF and wing-mounted DEP that utilize BLI. While the wing could support both technologies simultaneously, there would be impact on the effectiveness of each due to interference from the technologies. The team is currently investigating several DEP layouts to maximize the BLI benefit seen on the configuration. Computational results from this initial investigation are shown in “High Fidelity Computational Analysis and Optimization of the SUSAN Electrofan Concept” by L. Machado et al. [14]. The three layouts considered thus far include an upper-surface mount, a lower-surface mount, and a trailing-edge mount. Both the upper-surface and trailing-edge mounts have the upper surface boundary layer ingested into the engine. Initial studies show that if the engine is mounted with significant overlap on the upper surface, the aerodynamic impact of the BLI on the upper surface moves the shock significantly forward on the airfoil. A shock will cause boundary layer transition, so the introduction of the BLI system pushing the shock forward will reduce the possible extents of NLF and proportionately reduce the associated aerodynamic benefit. In addition to the limited extent of NLF due to shock movement, there are concerns that the engines could cause increased freestream turbulence levels due to noise or turbulence from the engine feeding forward and negatively impacting the extent of NLF. The DEP units are only distributed along the inboard portion of the wing, which would limit this reduction in NLF extent. Little impact is expected to the outboard extents of laminar flow where no DEP units are planned. In addition to the DEP systems possibly reducing the extent of NLF available, the use of NLF is expected to reduce the BLI benefit possible to these units. The performance benefit from a BLI engine is derived from ingesting the low-momentum flow in the boundary layer. Laminar flow reduces the thickness of a boundary layer, and would therefore reduce the amount of low-momentum flow going into the engine. Further studies are needed to estimate the potential reduction in BLI benefit resulting from a sustained length of laminar flow like those seen with CATNLF airfoils. Additionally, the DEP system would need to be robust enough to perform adequately while ingesting either a boundary layer associated with laminar flow (thinner) or fully-turbulent flow (thicker). While the configuration would be designed for significant extents of laminar flow, the engines would need to operate well in the off-design case that the flow is fully turbulent, such as if there is a surface imperfection or flight condition change resulting in loss of laminar flow. Additional studies are needed to identify the potential

difference in boundary layer thickness due to premature transition and the resulting impact on the performance of the DEP system.

The results presented here were focused on applying NLF to the main wing upper surface only. However, additional drag reduction is possible if laminar flow were supported on additional components. Future work may explore the performance increment associated with applying the CATNLF method to the tail surfaces or engine nacelles. Adding laminar flow to the tail or nacelle would have similar requirements for manufacturing and surface finishes. Crossflow suppression would be required on a tail surface due to the high component sweep, whereas a nacelle would only be focused on controlling TS growth. In order to be applied to tail surfaces, the CATNLF method would need to be altered to support symmetric or lightly-loaded pressure distributions since all the CATNLF applications thus far have been on a lifting wing. Further studies are needed to identify the compatibility of CATNLF technology with tail components.

V. Concluding Remarks

A promising new vehicle, referred to as the SUbsonic Single Aft eNgine (SUSAN) Electrofan, is being studied by a multidisciplinary team across several NASA centers. This new aircraft is in the conceptual design stage with several technologies being studied as possible additions to the vehicle. The primary new feature of the SUSAN Electrofan is the propulsion strategy, which is comprised of wing-mounted distributed electric propulsion and a single aft fuselage mounted turbofan engine. In addition to these novel propulsion techniques, the team is investigating the application of natural laminar flow to the main wing. This paper presents the computational study used to quantify the performance potential of implementing laminar flow, as well as discuss some multidisciplinary impacts of utilizing this technology.

To obtain laminar flow on the main wing, the Crossflow Attenuated Natural Laminar Flow (CATNLF) method was employed. This method uses airfoil shaping to obtain pressure distributions known to control the crossflow growth at the leading edge of components with high sweep and high Reynolds number, such as the main wing of the vehicle. For this study, laminar flow is only targeted on the wing upper surface because this provides the greatest drag reduction while still leaving the lower surface available for items such as leading edge high lift devices and maintenance access panels. To quantify the performance potential of laminar flow, two wing designs were conducted: a fully-turbulent design to represent the standard transonic cruise wing and a laminar design utilizing the CATNLF method. The laminar design supported laminar flow on 53% of surface area on the upper surface, which resulted in a 19-count (8.8%) drag reduction compared to the turbulent design. The laminar design performance benefit was maintained across near-cruise off-design conditions.

The high-fidelity designs presented in this paper are meant to serve as representations of the performance characteristics of the SUSAN Electrofan configuration if laminar flow is a final technology selected for the main wing. The final design would need to be performed on the full configuration with the wing-mounted distributed electric propulsion included, which is expected to have significant aerodynamic interference on the wing pressures. While these designs are on a simplified geometry, the effect of laminar flow on the performance of the vehicle was effectively studied and proved to be a promising technology to help the SUSAN Electrofan configuration meet its performance objectives.

Acknowledgments

This work was sponsored by the NASA Convergent Aeronautics Solutions (CAS) Project, which is part of the Transformational Aeronautics Concepts Program (TACP) in the NASA Aeronautics Research Mission Directorate (ARMD). Resources supporting some computational results in this paper were provided by the NASA High-End Computing (HEC) Program through the NASA Advanced Supercomputing (NAS) Division. The SUSAN Electrofan team is comprised of researchers across NASA Glenn Research Center, Ames Research Center, Langley Research Center, and Armstrong Flight Research Center.

References

[1] Jansen, R., Kiris, C., Chau, T., Machado, L., Duensing, J., Mirhashemi, A., Chapman, J., French, B., Miller, L., Litt, J., Denham, C., Lynde, M., Campbell, R., Hiller, B., Blaesser, N., and Heersema, N., "Subsonic Single Aft Engine (SUSAN) Transport Aircraft Concept and Trade Space Exploration", AIAA SciTech Forum, January 2021.

[2] Campbell, R. L., and Lynde, M. N., "Natural Laminar Flow Design for Wings with Moderate Sweep", 34th AIAA Applied Aerodynamic Conference, AIAA AVIATION Forum, AIAA 2016-4326, June 2016.

[3] Lynde, M. N. and Campbell, R. L., "Expanding the Natural Laminar Flow Boundary for Supersonic Transports", 34th AIAA Applied Aerodynamic Conference, AIAA AVIATION Forum, AIAA 2016-4327, June 2016.

[4] Lynde, M.N., Campbell, R.L., and Viken, S.A., "Additional Findings from the Common Research Model Natural Laminar Flow Wind Tunnel Test (Invited)," AIAA-2019-3292, June 2019.

[5] Lynde, M. N., Campbell, R. L., Rivers, M. B., Viken, S. A., Chan, D. T., Watkins, A. N., and Goodliff, S. L., "Preliminary Results from an Experimental Assessment of a Natural Laminar Flow Design Method", AIAA 2019-2298, January 2019.
[6] Rivers, M., Lynde, M., Campbell, R., Viken, S., Chan, D., Watkins, A., and Goodliff, S., "Experimental Investigation of the NASA Common Research Model with a Natural Laminar Flow Wing in the NASA Langley National Transonic Facility", AIAA 2019-2189, January 2019.
[7] Pandya, M. J., Jespersen, D. C., Diskin, B., Thomas, J. L., and Frink, N. T., "Efficiency of Mixed-Element USM3D for Benchmark Three-Dimensional Flows," AIAA Journal 2021, pp. 1-15.
[8] Campbell, R. L., "Efficient Viscous Design of Realistic Aircraft Configurations," AIAA-98-2539, June 1998.
[9] Wie, Y.-S., "BLSTA: A Boundary Layer Code for Stability Analysis," NASA CR 4481, 1992.
[10] Chang, C.-L., "The Langley Stability and Transition Analysis Code (LASTRAC): LST, Linear and Nonlinear PSE for 2-D, Axisymmetric, and Infinite Swept Wing Boundary Layers," AIAA 2003-0974, 2003.
[11] Poll, D.I.A., "Some Observations of the Transition Process on the Windward Face of a Long Yawed Cylinder," J. Fluid Mech., Vol. 150, 1985, pp. 329-356.
[12] Gaster, M., "A Simple Device for Preventing Turbulent Contamination on Swept Leading Edges," Royal Aero. Soc. J. Technical Notes, vol. 69, Nov. 1965, pp. 788-789.
[13] Wohl, C.J., Smith, Jr., J.G., Connell, J.W., Siochi, E.J, Penner, R.K., and Gardner, J.M., "Engineered Surfaces for Mitigation of Insect Residue Adhesion", AIAA 2013-0413, 2013.
[14] Machado, L.G., Chau, T., Kenway, G., Duensing, J.C., and Kiris, C.C., "High Fidelity Computational Analysis and Optimization of the SUSAN Electrofan Concept", AIAA SciTech Forum, January 2021.